

Supplement of

Wildfire plume ageing in the Photochemical Large Aerosol Chamber (PHOTO-LAC)

Hendryk Czech^{1,}, Olga Popovicheva^{2,*}, Dmitriy G. Chernov³, Alexander Kozlov⁴, Eric Schneider^{1,5}, Vladimir P. Shmargunov³, Maxime Sueur^{6,7}, Christopher P. Rüger^{1,5}, Carlos Afonso^{6,7}, Viktor Uzhegov³, Valerii S. Kozlov³, Mikhail V. Panchenko³, Ralf Zimmermann^{1,5}*

¹Joint Mass Spectrometry Centre (JMSC), Department of Analytical and Technical Chemistry, Chair of Analytical Chemistry, University of Rostock, 18059, Rostock, Germany

²Skobeltsyn Institute of Nuclear Physics, Lomonosov Moscow State University, 119991, Moscow, Russia

³V. E. Zuev Institute of Atmospheric Optics, Siberian Branch of the Russian Academy of Sciences, 634055, Tomsk, Russia

⁴Voevodsky Institute of Chemical Kinetics and Combustion, Siberian Branch of the Russian Academy of Sciences, 630090, Novosibirsk, Russia

⁵Department Life, Light & Matter (LLM), University of Rostock, 18059, Rostock, Germany

⁶Normandie Université, UNIROUEN, INSA Rouen, CNRS, COBRA, 76000, Rouen, France

⁷International Joint Laboratory – iC2MC: Complex Matrices Molecular Characterization, 76700, Harfleur, France

*corresponding authors: hendryk.czech@uni-rostock.de; olga.popovicheva@gmail.com

Table of Content

Table S1	Uncertainty of repeated APPI FT-ICR MS measurement
Fig. S1	Spatial homogeneity of temperature and relative humidity in PHOTO-LAC
Fig. S2	Coagulation and wall losses of particles for individual sizes
Fig. S3	Size distribution of fresh BB aerosol (flaming/smouldering)
Fig. S4	ePM and b_{abs} of flaming and smouldering BB aerosol during residence in PHOTO-LAC
Fig. S5	Wall loss of toluene
Fig. S6	Collision-induced dissociation (CID) of m/z 154 ($\text{C}_6\text{H}_4\text{NO}_4^-$)
Fig. S7	Evolution of ePM, NO, NO ₂ and O ₃ during dark ageing
Fig. S8	Venn diagrams of APPI high resolution mass spectra from long ageing experiments

Table S1 Repeated analysis of photochemically-aged BB aerosol (from BB6) with average and 95% confidence interval for the number of assigned sum formula, the modified aromaticity index (AI_{mod}), organic matter to organic carbon ratio (OM:OC) and elemental ratios H:C and O:C

	sum formula number	AI_{mod}	OM:OC	H:C	O:C
Analysis1	4314	0.37	2.44	1.31	0.15
Analysis2	4126	0.37	2.44	1.31	0.16
Analysis3	3368	0.38	2.43	1.29	0.17
Average	3936	0.38	2.44	1.30	0.16
95% CI	982	0.01	0.01	0.02	0.01

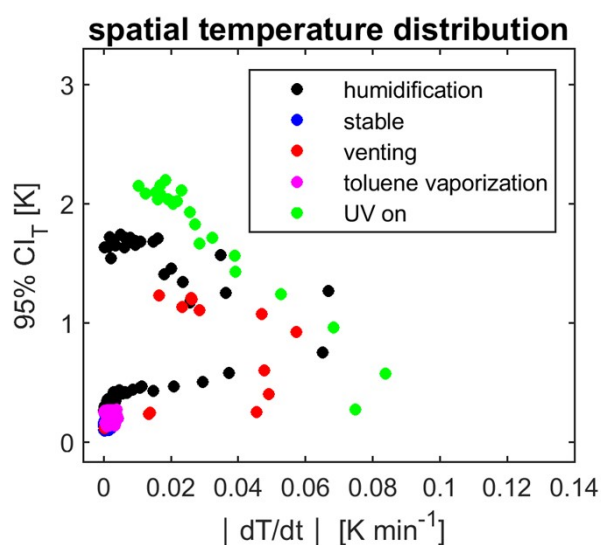
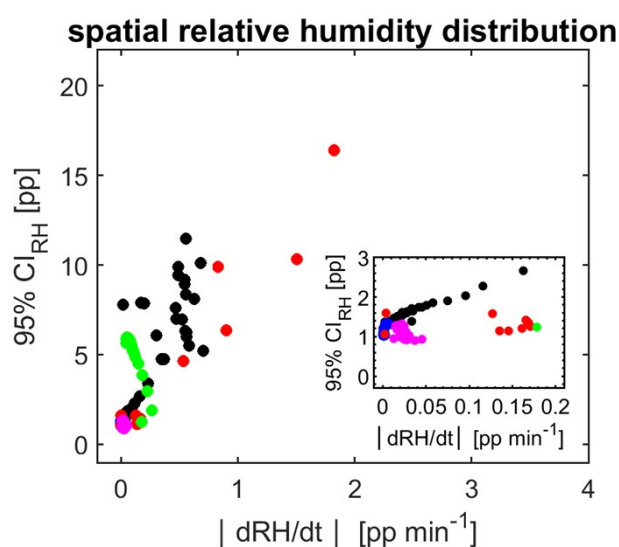


Fig. S1 95% Confidence interval (95% CI) of relative humidity (RH) and temperature (T) from twelve RH and T sensor measurements in PHOTO-LAC dependent on change over time for various operation conditions.

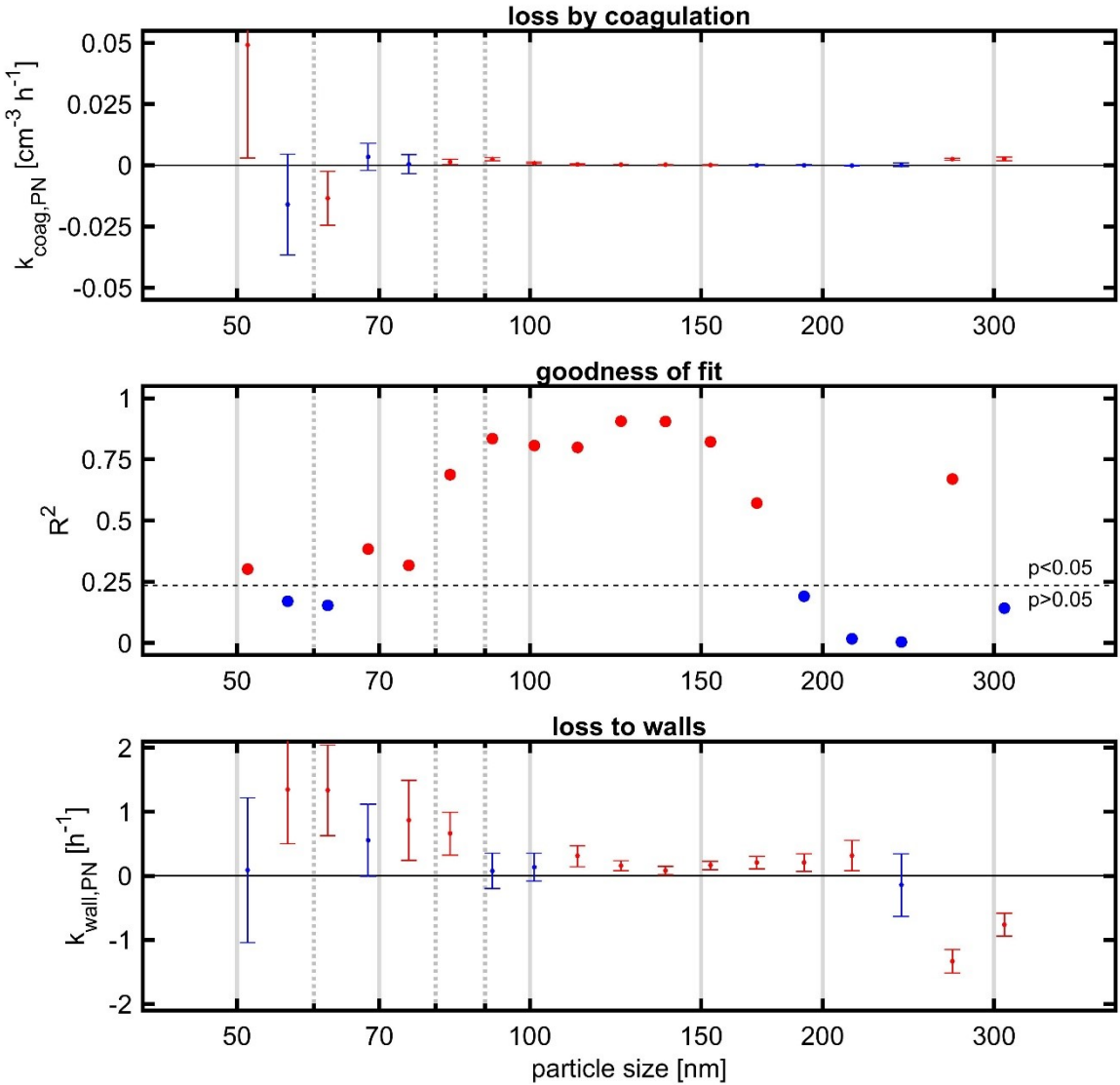


Fig. S2. Loss rate individual particle sizes due to coagulation or loss to the inner walls according to equation $dPN/dt = -k_{coag,PN} \cdot N^2 - k_{wall,PN} \cdot N$ with goodness of fit represented by explained variance R^2 between measured and fitted data. Red colour indicates statistically significant difference from zero at 5% level.

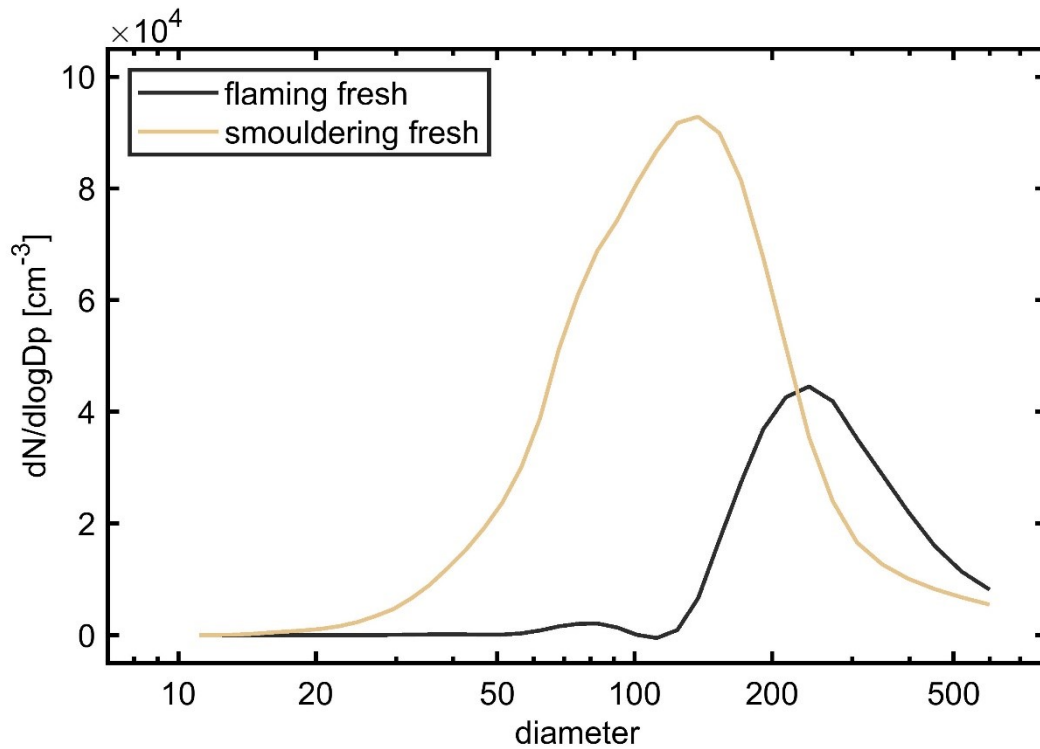


Fig.S3 Size distributions of fresh flaming and smouldering BB aerosol from experiments BB1 and BB6 referring to Table 1 of the main manuscript.

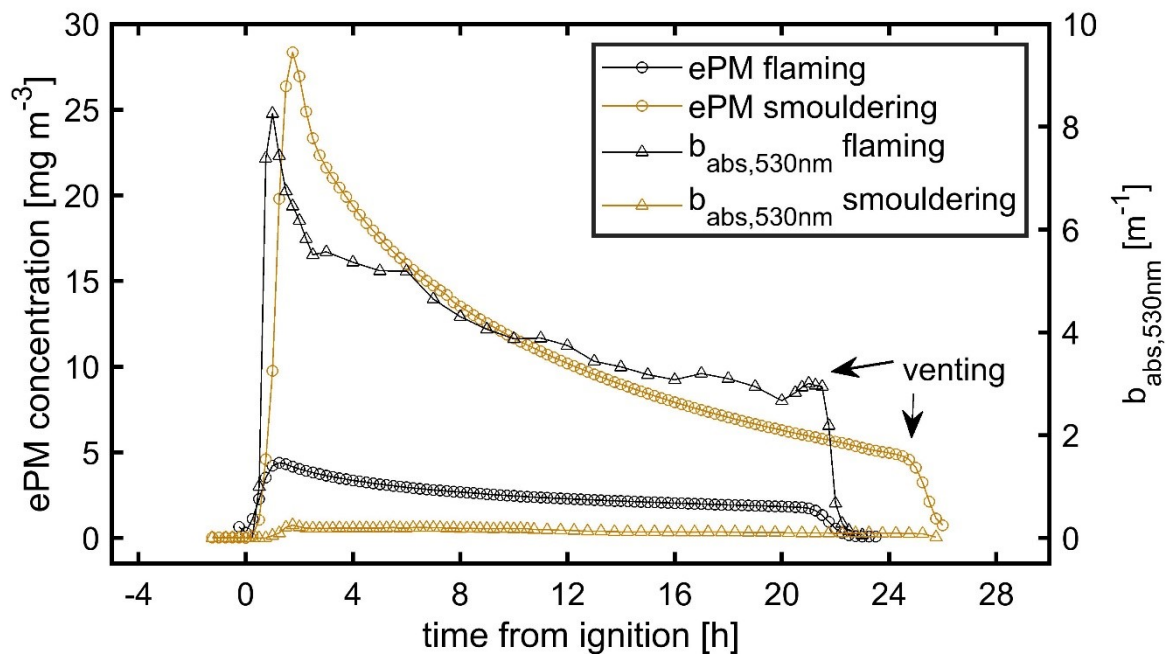


Fig. S4. ePM and b_{abs} from BB under flaming (black) and smouldering (brown) conditions derived from nephelometer (circles) and aethalometer at 530 nm (triangles). Declining concentrations of flaming aerosol after 22 h and smouldering aerosol after 25 h results from PHOTO-LAC venting.

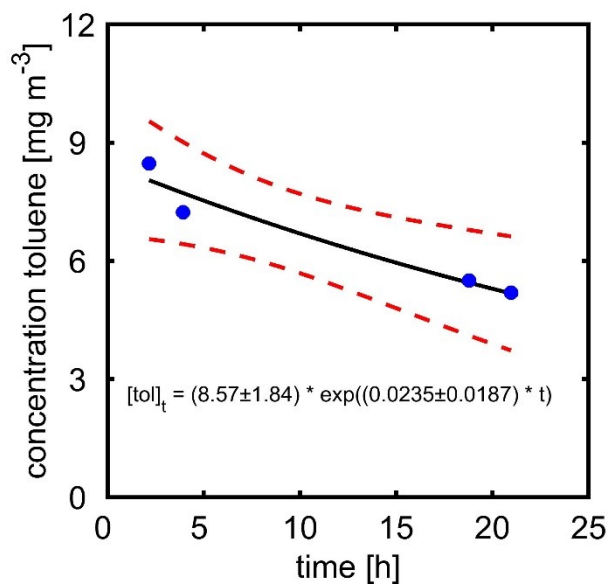


Fig. S5. Toluene loss over time with 95% non-simultaneous functional confidence band.

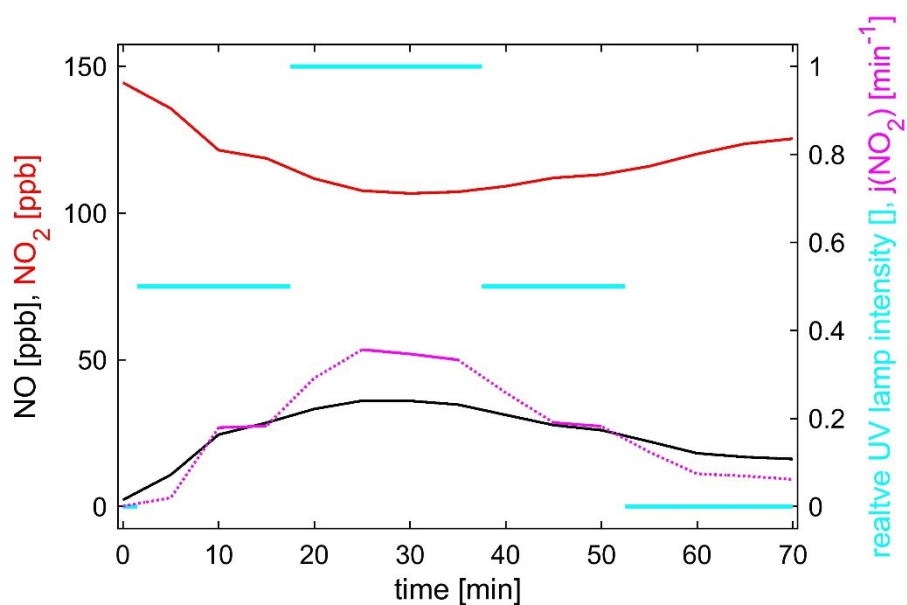


Fig. S6. Temporal concentrations of NO and NO₂ at 50% and 100% UV light intensity. The final photolysis rate $j(\text{NO}_2)$ was obtained from periods indicated by solid lines.

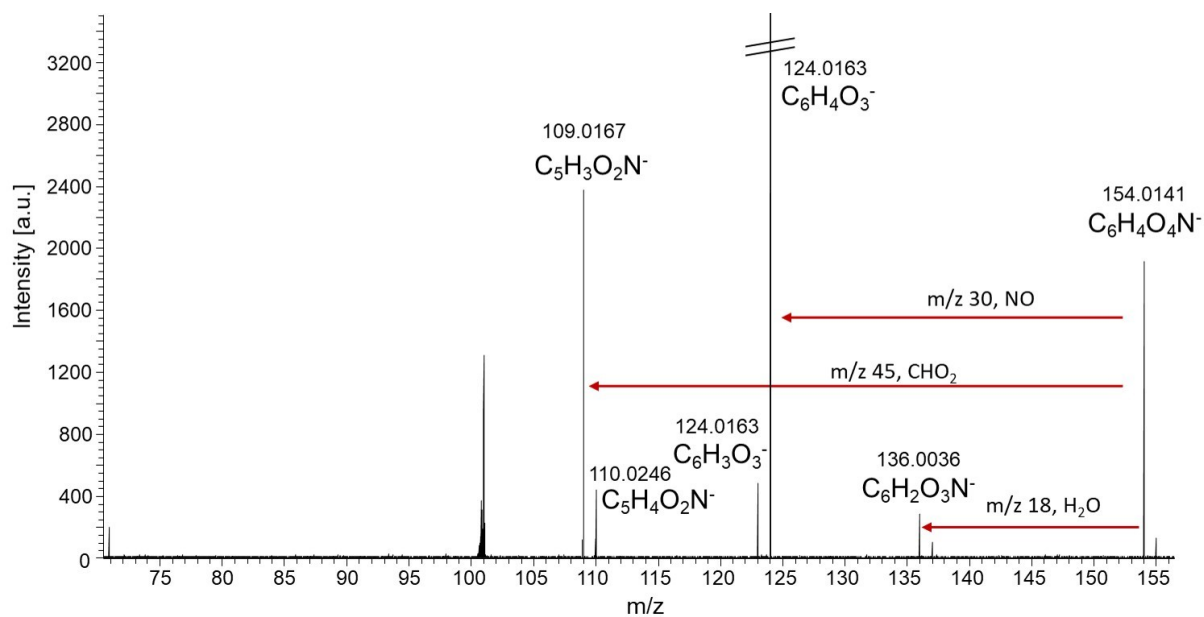


Fig. S7. Collision-induced dissociation (CID) of m/z 154 in aerosol from toluene photooxidation (tol4). The most intense fragment was observed at m/z 124.016 corresponds to NO neutral loss, indicating the presence of 4-nitro-catechol. The signal at m/z 101 belong to electronic noise.

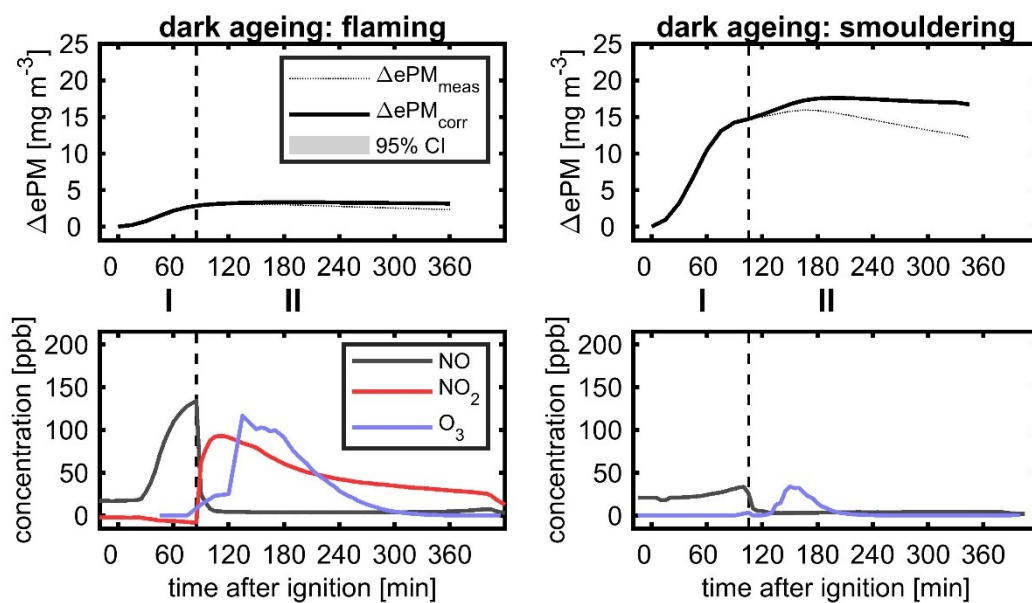


Fig. S8 short dark ageing of flaming (left) smouldering BB aerosol (right) with temporal evolution of equivalent particle mass (ePM; top) and gases NO, NO₂ and O₃ (bottom) for (I) generation of BB aerosol and (II) ozone addition. In order to facilitate formation of $\cdot\text{NO}_3$, after conversion of NO to NO₂ the same amount of O₃ is added 30 min later. For smouldering condition, no NO₂ data is available.

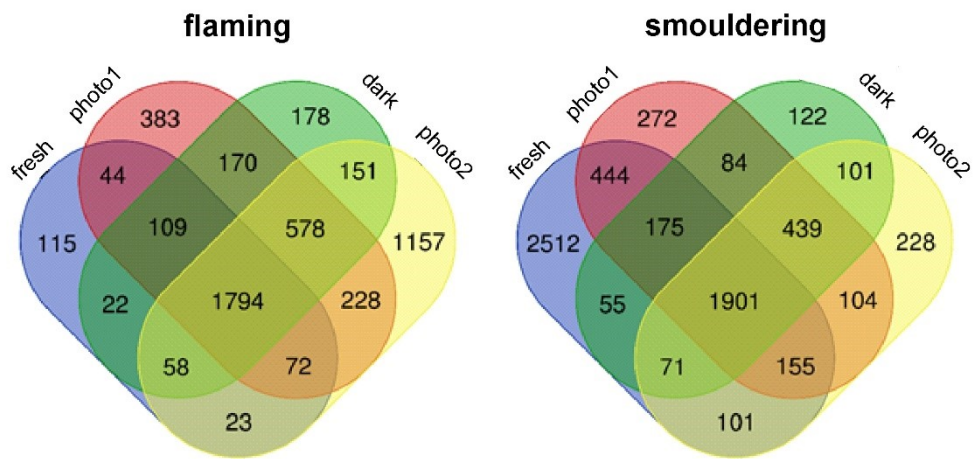


Fig. S9. Venn diagrams of APPI high resolution mass spectra from long ageing with alternating photochemical (photo1 and photo 2) and dark ageing (dark) conditions.